Space Weather Research in Greece: The Solar Energetic Particle Perspective

Olga E. Malandraki

IAASARS, National Observatory of Athens, GR-15236, Pedeli,
Greece National Coordinator, International Space Weather Initiative (ISWI)

Email (omaland@astro.noa.gr)

Accepted: 18 December 2014

Abstract. Space Weather Research carried out in the National Observatory of Athens (NOA), within the SEPServer and COMESEP projects under the Seventh Framework Programme (FP7-SPACE) of the European Union (EU) is presented. Results and services that these projects provide to the whole scientific community as well as stakeholders are underlined. NOA strongly contributes in terms of crucial Solar Energetic Particle (SEP) dataset provided, data analysis and SEP catalogue items provided as well as comparative results of the various components of the project server, greatly facilitating the investigation of SEPs and their origin. SEP research highlights carried out at NOA are also presented, used to test and validate the particle SEP model developed and incorporated within the SEP forecasting tools of the COronal Mass Ejections and Solar Energetic Particles (COMESEP) Space Weather Alert System, i.e. the First European Alert System for geomagnetic storms and SEP radiation hazards.

Keywords: Solar eruptive events, Solar Energetic Particles, Coronal Mass Ejections, solar flares, Space Weather Alerts

Introduction

Solar Energetic Particle (SEP) events are a key ingredient of solar-terrestrial physics both for fundamental research and space weather applications. SEP events, are the defining component of solar radiation storms, contribute to radio blackouts in polar regions and are related to many of the fastest Coronal Mass Ejections (CMEs) driving major geomagnetic storms. In addition to CMEs, SEP events are also related to flares (e.g. Reames, 2013). The occurrence rate of large, space-weather relevant SEP events is about 100 per solar cycle, with a broad distribution in time that extends well into the declining phase of the activity cycle as traced by the sunspot index.

The SEPserver and COMESEP projects have been two three year collaborative projects funded under the Seventh Framework Programme (FP7-SPACE) of the European Union (EU) and coordinated by the University of Helsinki in Finland and the Belgian Institute for Space Aeronomy in Belgium, respectively. NOA in Greece participates as a Collaborating Partner in both the SEPServer and COMESEP projects.

The SEPServer project provides a new tool, which greatly facilitates the investigation of SEP events and their origin. This is achieved via an internet server (http://server.sepserver.eu) which gives access to a large number of SEP datasets from different instruments onboard several missions, to Electromagnetic (EM) observations related to the events identified from the SEP data and to state-of-the art analysis tools that can be used to infer the solar SEP emission time profiles and interplanetary transport conditions prevailing during the SEP events. Furthermore, the project provides analysis results on the events in the form of comprehensive catalogs that list key properties of the events. It also led to better understanding of the particle acceleration and transport processes at the Sun and in the inner heliosphere, resulting to SEP events that form one of the key elements of space weather.

The COronal Mass Ejections and Solar Energetic Particles (COMESEP) project has developed tools for forecasting geomagnetic storms and SEP radiation storms. By analysis of historical data, complemented by the extensive data coverage of solar cycle 23, the key ingredients that lead to magnetic storm and SEP events and the factors that are responsible for false alarms have been identified. The structure, propagation and evolution of CMEs have been investigated, enhancing our understanding of the 3-D kinematics and interplanetary propagation of CMEs. In parallel, the sources, acceleration and propagation of SEPs have been examined and modelled. COMESEP is a unique cross-collaboration effort and bridges the gap between the SEP, CME and terrestrial effects scientific communities.

In this paper, we present a review of the Space Weather research, results and contributions from the SEP perspective, carried out at NOA in Greece within the SEPServer and COMESEP projects.

SEPServer SEP Data, Catalogs and Research

In coordination with the Principal Investigator (PI) teams in the US and Europe, NOA directly contributes to SEPServer the electron, ion and heavy ion datasets of the Electron, Proton, and Alpha Monitor (EPAM) (Gold et al., 1998) and the Solar Isotope Spectrometer (SIS) (Stone et al., 1998) instruments onboard the Advanced Composition Explorer (ACE), the particle datasets of the Heliosphere Instrument for Spectra, Composition and Anisotropy (HI-SCALE) (Lanzerotti et al., 1992) and the Cosmic Ray and Solar Particle Investigation/ Low Energy Telescope (COSPIN/LET)

(Simpson et al., 1992) experiments onboard Ulysses as well as the proton dataset of the Low-Energy Telescope (LET) instrument (Mewaldt et al., 2008) onboard both the twin STEREO spacecraft. Important documentation on these datasets, such as reports on the assessment of their quality accompanying each dataset was also provided by NOA.

One of the most important scientific conclusions of the SEPServer project is the implementation and release to the SEP community of multiple SEP event catalogues based on different spacecraft and instruments, covering a broad timescale from 1975 to 2012 as well as a variety of radial distances from 0.3 to ~5 AU in the 3-Dimensional Heliosphere. In particular, SEPServer hosts six catalogues of SEP events based on observations from the SOHO, Ulysses, Helios-A & B and STEREO A & B spacecraft.

SOHO/ERNE Catalogue

The first SEPServer catalogue (Vainio et al., 2013) is based upon the systematic scan of ~68 MeV proton intensities observed at 1 AU in 1996-2010. This proton energy was purposely chosen considered appropriate for the goals of the SEPServer project from the point of view of space weather relevance. A total of 115 solar proton events for the 23rd solar cycle were identified using data from the Energetic and Relativistic Nuclei and Electron (ERNE) experiment onboard the Solar and Heliospheric Observatory (SOHO). Parallel scanning has been performed at NOA of the electron recordings of the ACE/EPAM experiment during the identified events, and the onset time of the events in the 0.18-0.31 MeV channel has been determined. The algorithm determines the average intensity I and the standard deviation σ inside the specified time window and then compares the data just ahead of this window with a threshold I + nσ, where n can be chosen by the user (3σ are used for EPAM). The onset is defined as the time stamp of the first point above the threshold (Malandraki et al., 2012). The onset time of each event was determined and then a time-shifting analysis (TSA) of the onset times was performed to get the Solar Release Time (SRT) of the electrons at the Sun, which were included and presented in the first SEPServer catalogue. The anticipated SRT from ACE/EPAM measurements is based on the assumption that the velocity vector of the first arriving particles constitutes an angle of 0° with the vector of the magnetic field. For each event, using the measured solar wind speed by the ACE/SWEPAM experiment (McComas et al., 1998) at the time of the onset of the electron event, the nominal length of the Parker spiral L connecting Earth to the Sun was numerically calculated (Malandraki et al., 2002; Vainio et al., 2013). Another important information that NOA contributed to this catalogue is a qualitative description of the electron anisotropy as observed by EPAM (e.g. beam, moderate, isotropic Pitch-Angle Distributions, PADs). This gives an indication of how much scattering is experienced by electrons during interplanetary transport (e.g. Dresing et al., 2014). The events with beam-like anisotropy can be regarded as those with the most reliable SRT. It should be noted that we have added 500 sec i.e. the light travel time per AU to the release time of the channel to allow an easier comparison with EM emission observations at 1 AU.

Ulysses/COSPIN/KET Catalogue

The second SEPServer catalogue (Heber et al., 2013) is based upon the systematic scan of proton intensities of 32 MeV < E < 125 MeV and in parallel the highest energy channel in the energy range 125 MeV < E < 250 MeV of the COSPIN/Kiel Electron Telescope (KET) instrument onboard the Ulysses spacecraft for a time period from 1998-2009 (end of Ulysses mission). A total of 40 proton events were identified in the 3-dimensional heliosphere over solar cycle 23 using data from COSPIN/KET. The EPAM instrument is the flight spare of the HI-SCALE experiment and practically identical to it. We performed at NOA parallel scanning of the electron measurements by the HI-SCALE experiment onboard Ulysses during the identified events and we carried out onset time determination analysis in the 0.18-0.31 MeV channel as well as TSA to derive the anticipated SRT of the particles at the Sun using a similar algorithm as for the EPAM data for the SOHO/ERNE catalogue events. NOA also contributed a qualitative description of the electron PADs taking advantage the available sectored data of the spinning spacecraft. All this scientific analysis has been tabulated and included in this second SEPServer catalogue.

Helios A & B Catalogues

For the production of the third and fourth SEPServer catalogues the E6 experiment on board both Helios spacecraft (Helios-A & Helios-B) was used. The Helios (A or B) catalogues are based on the systematic scan of proton intensities at 37 MeV, with a parallel scanning of the integral proton intensities at > 51 MeV and electrons at > 2 MeV covering a time period from 1975-1982 (for Helios A) and 1977-1980 (for Helios B; Malandraki et al., 2013). It should be noted that these Catalogues are very important also in the context of the future solar mission 'Solar Orbiter' of the European Space Agency (ESA) that is foreseen to be launched in 2017 and will explore the inner heliosphere with experiments of unprecedented capabilities. NOA participates to the Solar Orbiter/EPD (Energetic Particle Detector) experiment at a Co-Investigator Level (Dr. Olga Malandraki, NOA).

STEREO - A & B Catalogs

The fifth and sixth catalogues of SEPServer were compiled based on the recordings of the STEREO-A and B (STA & STB) twin spacecraft, during the descending phase of the solar cycle 23 and the rising phase of solar cycle 24, from 2007 to 2012. First, we, at NOA, made a complete survey of the 10-min averaged low energy proton intensities within the energy range 6-10 MeV from the LET instrument from 2007-2012 for both spacecraft. Figure 1 illustrates the methodology that was applied to the LET data leading to the identification of the possible candidate for the SEP events (Papaioannou et al., 2014). 1-day averaged

intensities of 6-10 MeV protons recorded at LET vs. time from 2007 until the end of 2012 are presented in both panels. The quite-time background level is presented in both panels with a straight line, red in the case of STA (bottom panel) and blue in the case of STB (upper panel). We thus spotted all enhancements above the quite-time background level of LET and listed them as possible candidate for SEP events. No other intensity threshold restriction (e.g. the criterion of the intensity exceeding at least one order of magnitude above the background intensity during the SEP event) was applied so that we could ensure that even the smallest SEP events would be identified and included in these catalogues. This meticulous scanning for the identification of the possible SEP events led to the inclusion of all candidate SEP events while excluding none.

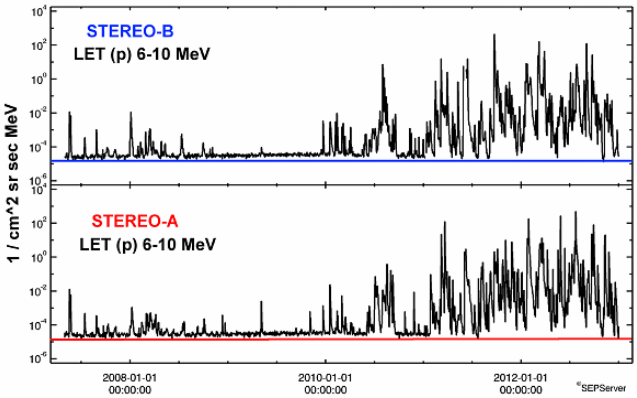

Figure 1: Daily averaged LET proton intensity profiles at the STA and STB spacecraft from 2007 until the end of 2012 vs. time. (Papaioannou et al., 2014). This figure was created at SEPServer (http://server.sepserver.eu).

A significant number of the identified particle enhancements could possibly be related to Corotating Interaction Regions (CIRs) and/or Stream Interaction Regions (SIRs, Malandraki et al., 2007; Gómez-Herrero et al., 2011). In order to exclude such cases, we carried out an extensive literature survey and found works which targeted for the identification of CIRs as well as works with single case SEP studies in the STEREO era (e.g. Leske et al., 2011; Bucík et al., 2009), which allowed us to clear up our initial sample of enhancements, by using the results of this literature survey as a first estimate for the presence or absence of a CIR enhancement in our tabulated candidate sample of enhancements. Furthermore, we have cross-correlated our initial sample of enhancements to the identified intervals that SIRs were observed at both STEREO spacecraft, based on the SIRs catalogs identified by STEREO, maintained by the Space Physics Center at the University of California (UCLA). We also carried out cross correlations to available lists of shocks in order to spot if the recorded tabulated enhancements were shock related enhancements. Moreover, we made a parallel scanning of high time resolution near-relativistic electron recordings from the STEREO/Solar Electron Proton Telescope (SEPT) instrument in order to identify which of our initial candidate enhancements tabulated as possible SEP events also presented an electron signature in SEPT, since the ratio of protons-to-electrons varies in CIRs, with electron events being rare and proton events relatively common (e.g. Richardson, 2004). In addition we also scanned the recordings of the High Energy Telescope (HET) onboard STEREO from 40-100 MeV, in order to identify which of the events in our catalogues extend to high energies and thus were the most space weather relevant ones. Using the above methodology we have identified at NOA 130 SEP events for STA and 108 SEP events for STB (Tables 1-4 in Papaioannou et al., 2014). The onset, peak time and peak intensity value of each SEP event for LET 6-10 MeV protons as well as for SEPT 55-85 keV electrons have been determined and included in these online catalogues. An example of the actual online layout of the SEPServer STEREO catalogues is shown in Figure 2. The user of SEPServer has direct access to the information for each event in both textual and graphical form. TSA has been performed for the electron measurements using the solar wind speed as measured by the PLASTIC instrument onboard STEREO (Galvin et al., 2008). The relevant solar associations in terms of EM emissions are also provided as well as a list of a subset of events with clear recordings at both STEREO spacecraft and the parent solar events of these multi-spacecraft SEP events.

First comparative results of SEPServer - the 13 July 2005 event case study

Malandraki et al. (2012) presented the first comparative results of the SEPServer project through the scientific analysis carried out for the case study 13 July 2005 event, demonstrating the new perspectives that are made available to the SEPServer users. Data-driven analysis and simulation-based data analysis capable of deconvolving the effects of interplanetary transport and solar injection from SEP observations were carried out and the results were compared directly with the EM emission signatures. Figure 3 presents the time evolution of the both electron and proton profiles as observed by different instruments. The onset of the SEP event under study is marked by a dashed vertical line in this Figure. For this event Velocity Dispersion Analysis (VDA) using the Poisson-CUSUM algorithm (Huttunen-Heikinmaa, Valtonen, and Laitinen, 2005) at 17 energy channels of the SOHO/ERNE instrument was carried out and provided the SRT of 14:31 UT ± 15 min and the apparent path length of 2.84 ± 0.19 AU. The results of the VDA are presented in Figure 4 (upper panel), where the onset time of the proton event observed in each energy channel as a function of the proton inverse velocity of the mean energy of each channel is shown. We have also used electron measurements by the Semi Conductor Detector Telescope (SST) of the Plasma and Energetic Particle Investigation (3DP) experiment (Lin et al. 1995) onboard the WIND spacecraft in the energy range 25-650 keV and estimated the onset time in each energy channel using

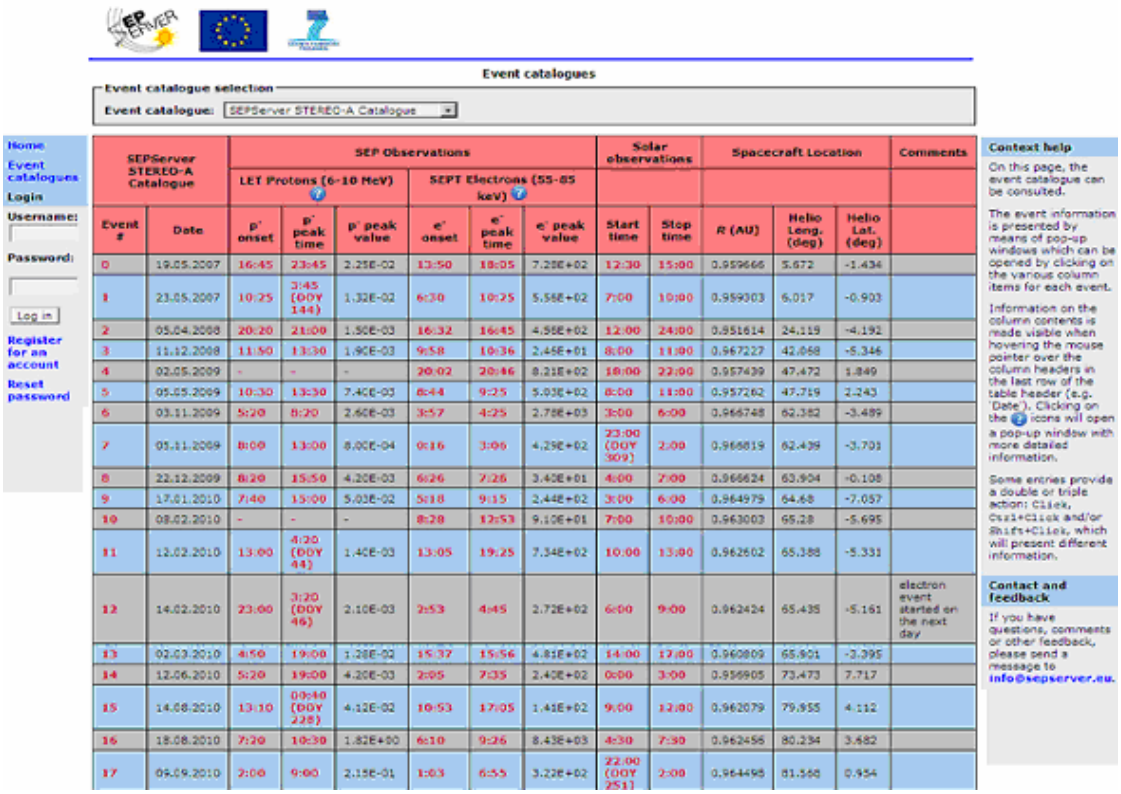

Event catalogues

Event catalogue selection

Event catalogue: SEPServer STEREO-A Catalogue

Home | Event catalogues | Login | Username: | Password: | Log in | Register for an account | Reset password

SEPServer STEREO-A Catalogue		SEP Observations						Solar observations		Spacecraft Location			Comments
		LET Protons (6-10 MeV)			SEPT Electrons (55-85 keV)								
Event #	Date	p onset	p peak time	p peak value	e onset	e peak time	e peak value	Start time	Stop time	R (AU)	Helio Long. (deg)	Helio Lat. (deg)	
0	19.05.2007	16:45	23:45	2.25E-02	13:50	18:05	7.28E+02	12:30	15:00	0.959666	5.672	-1.434	
1	23.05.2007	10:25	3:45 (DOY 144)	1.32E-02	6:30	10:25	5.56E+02	7:00	10:00	0.959003	6.017	-0.903	
2	05.04.2008	20:20	21:00	1.50E-03	16:32	16:45	4.56E+02	12:00	24:00	0.951614	24.119	-4.192	
3	11.12.2008	11:50	13:30	1.90E-03	9:58	10:36	2.45E+01	8:00	11:00	0.967227	42.068	-5.346	
4	02.05.2009	-	-	-	20:02	20:46	8.21E+02	18:00	22:00	0.957439	47.472	1.849	
5	05.05.2009	10:30	13:30	7.40E-03	8:44	9:25	5.03E+02	8:00	11:00	0.957262	47.719	2.243	
6	03.11.2009	5:20	8:20	2.60E-03	3:57	4:25	2.78E+03	3:00	6:00	0.966748	62.382	-3.489	
7	05.11.2009	8:00	13:00	8.00E-04	9:16	3:06	4.29E+02	23:00 (DOY 309)	2:00	0.966819	62.439	-3.701	
8	22.12.2009	8:20	15:50	4.20E-03	6:26	7:26	3.40E+01	4:00	7:00	0.966624	63.904	-0.108	
9	17.01.2010	7:40	13:00	5.03E-02	5:18	9:15	2.44E+02	3:00	6:00	0.964979	64.68	-7.057	
10	08.02.2010	-	-	-	8:28	12:53	9.10E+01	7:00	10:00	0.963003	65.28	-5.695	
11	12.02.2010	13:00	4:20 (DOY 44)	1.40E-03	13:05	19:25	7.34E+02	10:00	13:00	0.962602	65.388	-5.331	
12	14.02.2010	23:00	3:20 (DOY 46)	2.10E-03	2:53	4:45	2.72E+02	6:00	9:00	0.962424	65.435	-5.161	electron event started on the next day
13	02.03.2010	4:50	19:00	1.28E-02	15:37	15:56	4.81E+02	14:00	17:00	0.960809	65.901	-3.395	
14	12.06.2010	5:20	19:00	4.20E-03	2:05	7:35	2.40E+02	0:00	3:00	0.956905	73.473	7.717	
15	14.08.2010	13:10	00:40 (DOY 228)	4.12E-02	10:53	17:05	1.41E+02	9:00	12:00	0.962079	79.955	4.112	
16	18.08.2010	7:20	10:30	1.82E+00	6:10	9:26	8.43E+03	4:30	7:30	0.962456	80.234	3.682	
17	09.09.2010	2:00	9:00	2.15E-01	1:03	6:55	3.22E+02	22:00 (DOY 251)	2:00	0.964498	81.568	0.954	

Context help

On this page, the event catalogue can be consulted.

The event information is presented by means of pop-up windows which can be opened by clicking on the various column items for each event.

Information on the column contents is made visible when hovering the mouse pointer over the column headers in the last row of the table header (e.g. 'Date'). Clicking on the icons will open a pop-up window with more detailed information.

Some entries provide a double or triple action: Click, Ctrl+Click and/or Shift+Click, which will present different information.

Contact and feedback

If you have questions, comments or other feedback, please send a message to info@sepserver.eu.

Figure 2 Snapshot of the actual online layout of the STEREO catalogs (Papaioannou et al., 2014).

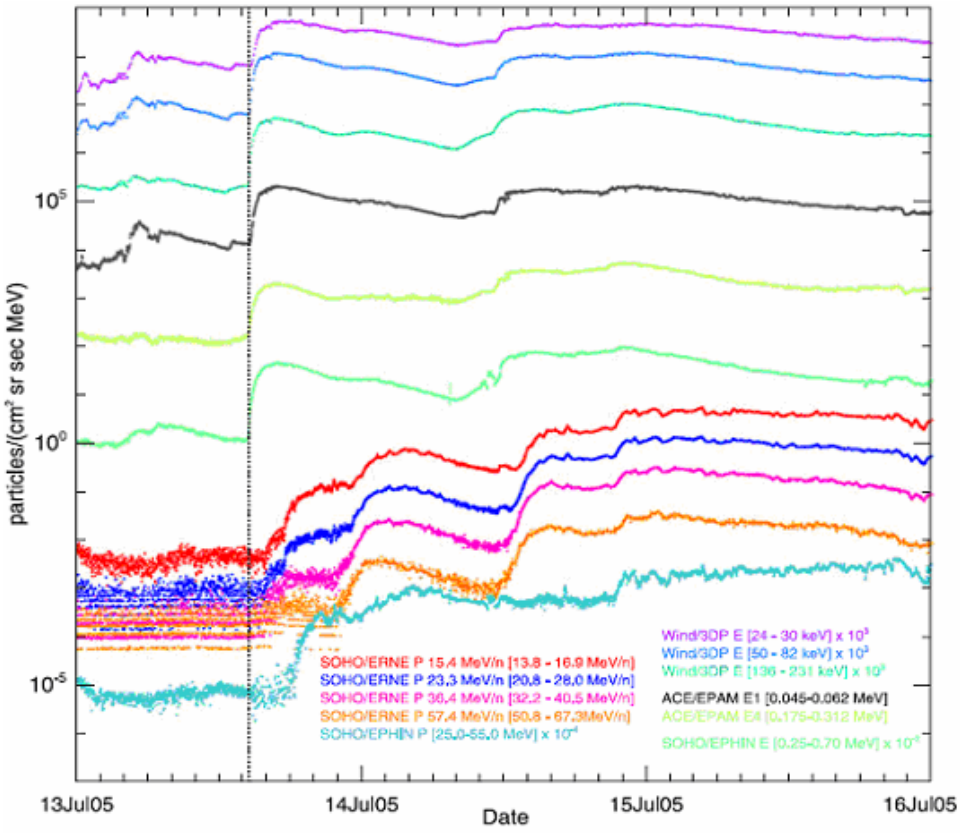

Figure 3 Electron and proton observations from 13-16 July 2005. The dashed line indicates the onset of the event at 14:30 UT, approximately (Malandraki et al., 2012).

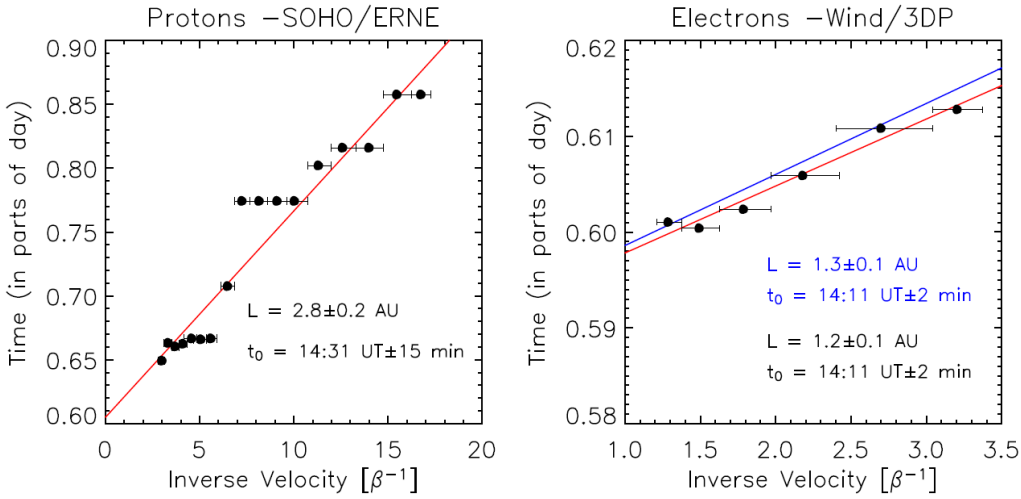

Figure 4 Onset times of the proton event observed by SOHO/ERNE (upper panel) and the electron event observed by Wind/3DP (bottom panel) as a function of inverse velocity. The blue line indicates the VDA results by Wind/3DP taking the high-energy limit of the channels as a reference (see text for details).

the Poisson-CUSUM method. Using VDA,we obtained an electron apparent path length L = 1.2 ± 0.1 AU and a SRT t_o = 14:11 UT ± 2 min as shown in Figure 4 (lower panel). The blue line indicates the electron VDA results taking the high-energy limit of the energy channels as a reference. The onset times for ACE/EPAM and SOHO/EPHIN were determined using the σ method (as previously described in detail in the 'SOHO/ERNE catalogue' subsection and were found to be 14:33 UT (for the 0.175-0.312 MeV electron channel) and 14:27 UT (for the 0.25-0.70 MeV electrons) respectively. The corresponding electron SRT for ACE/EPAM was calculated using TSA and identified to be 14:29 UT (adding 500 s for direct comparison with EM observations at 1 AU).

The time history of X-ray and radio emissions associated with the 13 July 2005 SEP event is shown in Figure 5. The panel displays, from bottom to top, the time profiles of soft X-ray in two wave bands (GOES satellites, NOAA), hard X-ray count rates in two photon energy ranges observed by the INTEGRAL/ACS and RHESSI instruments, radio spectrum at dm-m waves (ARTEMIS spectrograph), one-dimensional brightness, projected on to the solar east-west direction (Nancay Radioheliograph, NRH) between the center of the solar disk (0) and 2 R_s west of it, decametric-to-kilometric wave spectrum (Nancay Decameter Array (NDA), and Wind/WAVES radio spectrograph). The horizontal arrow above the plots and the two vertical lines mark the time interval of solar proton release inferred from the velocity dispersion analyses of the SOHO/ERNE measurements (Figure 4).

We modeled the 13 July 2005 electron event using measurements from the Wind/3DP plasma and energetic particle experiment, making use of simulations of the interplanetary transport of SEPs,

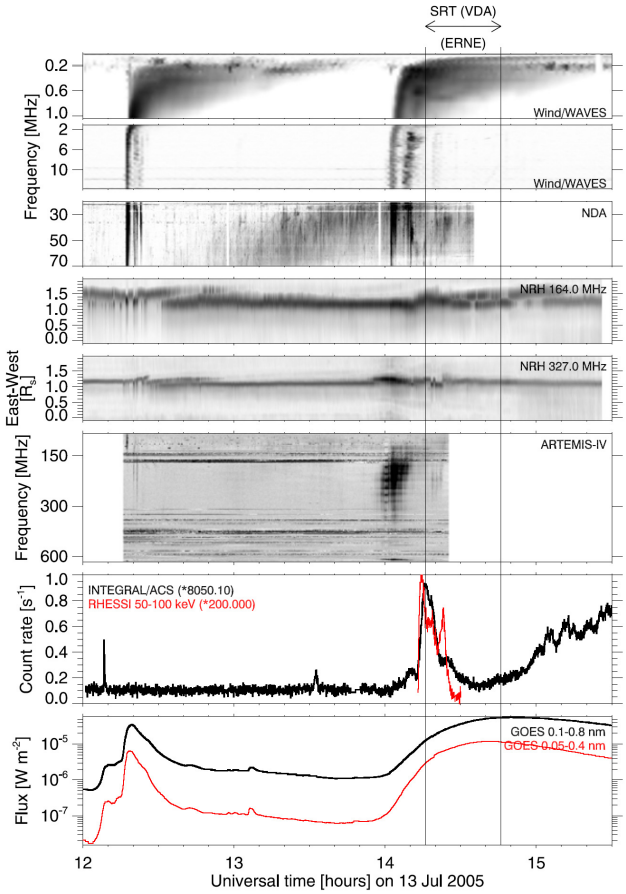

Figure 5 Time history of radio and X-ray emission before and near the onset of the SEP event on 13 July 2005. The horizontal arrow above the plots and the two vertical lines mark the time interval of solar proton release inferred from the velocity dispersion analyses of the SOHO/ERNE measurements.

followed by optimization of injection and transport parameters.

The quantitative treatment of the evolution of the particles' phase space density can be described by the focused transport equation (FTE) (Roelof, 1969). We used three different techniques to model the particle transport: a Finite Differences (FD) model (Dröge, 2003) that solved the FTE at a fixed particle energy, but has the advantage of being fast (~1 min for 1 run) and two Monte Carlo models (Kartavykh et al., 2007; Agueda et al., 2008) to solve the corresponding stochastic differential equations (SDEs) for an energy range adjusted to the width of the instrument channel under consideration.

As usual, these models assume an Archimedean spiral magnetic flux tube connecting the Sun and the spacecraft, consistent with the solar wind speed measured in situ. As initial conditions, electrons are released close to the Sun at 10 and 2 solar radii respectively), following a power law in energy in the Monte Carlo models. The results of the models are intensity directional distributions of electrons at the spacecraft location resulting from an instantaneous injection close to the Sun, i.e. they provide the Green functions of interplanetary transport. Figure 6 (top part) shows the omnidirectional intensity and anisotropy-time profiles observed by WIND/3DP on 13 July 2005. Two different fits are shown both obtained by the 'eye-ball' fit method. In one case, the solution of a Monte Carlo transport model in the 50-82 keV energy range is used while in the other a FD model is employed to solve the transport equation at the fixed energy of 66 keV. In both cases, the omnidirectional intensity and the first order anisotropy were tried to be simultaneously fit by means of varying the injection parameterization and the interplanetary transport conditions. As shown in Figure 6, the transport parameters obtained from the two fits are very similar a parallel mean free path λ_r = 0.06 AU for the MC model and λ_r = 0.07 AU for the FD model. An instantaneous injection at 14:06 UT is deduced using the Monte Carlo model, while a slightly longer injection is deduced from the FD model, starting at 14:04 UT.

We have inferred that the SRT of the first near-relativistic electrons occurs 20 min before that of the energetic protons. We cannot say if the difference of early release times of protons and electrons is a significant and systematic feature. However, it should be pointed out that such differences have been found in previous studies using Helios data (Kallenrode and Wibberenz, 1991) and occasional findings have been reported (Krucker and Lin, 2000) where different path lengths were inferred from VDA of near-relativistic electrons and for protons at MeV energies. SEPServer aims at providing the data and tools necessary for comprehensive studies, using multiple spacecraft and complementary methods of analysis including interplanetary propagation.

Inspection of the calculated electron PADs as measured by the ACE/EPAM instrument revealed that moderate anisotropic characteristics are observed after the onset of the event, which strongly implies scattering of the energetic particles in the Interplanetary (IP) space. The onset time of the event using ACE/EPAM and SOHO/EPHIN measurements has been determined at ~14:30 UT for the electrons. The VDA analysis of WIND/3DP electrons provided a SRT of 14:19 UT (adding 500 s for comparison reasons) and is in good agreement with the associated EM solar emission observations (Figure 5), which showed that intense type III radio burst, denoting solar electron release into open Interplanetary Magnetic Field (IMF) lines, occur from at 14:00 UT onwards. Based on the fitting of the intensity and anisotropy time profiles observed, short mean free paths were derived for the electrons, denoting that they experienced significant scattering, which is in agreement with the observed PADs from ACE/EPAM which showed moderately anisotropic characteristics (Malandraki et al., 2012). The main result of the simulation analysis is that during this SEP event several impulsive injections take place, in close association with the aforementioned Decametric-Hectometric type III Radio Bursts (RBs) starting at 14:10 UT and persistently observed afterwards, with the first prompt electron injection episode lasting from14:05-14:16 UT (having added 500 s for comparing to the EM emissions) representing the ~78% of the total injected particle population (Figure 7). The latter result is also in a reasonable agreement with the results of the data-driven analysis.

Space Weather Research Activities within the COMESEP project

SEP events have been previously studied extensively in the 3-dimensional (3-D) heliosphere (Malandraki et al., 2008; Malandraki et al., 2009). For COMESEP, study of the intensity characteristics and angular distributions for SEP events was carried out at NOA in order to assess the impact of the large-scale IMF structure on the SEP time profiles. This is important in space weather forecasting e.g. a reflecting boundary that blocks a flux tube (Malandraki et al., 2002) is important since it can lead to the reservoir effect (Roelof et al., 1992) thus extending the duration of the space weather hazard. Furthermore, we investigated the path length difference between solar electrons and ions in the Ground Level Enhancement (GLE) events in solar cycle 23, using data from the Wind spacecraft. The observed similarities and differences in the spectral and compositional signatures have also been investigated to shed light on the SEP sources, and acceleration processes operating on the SEPs in terms of solar flares, CMEs and their driven propagating shocks in the interplanetary medium. The mechanisms leading to the latitudinal spread of SEP in the heliosphere were also investigated. All these results were used in order to test and validate the test particle SEP model developed, representing valuable input for the SEP forecasting tools and are incorporated within the COMESEP Space Weather Alert System (Crosby et al., 2012; www.comesep.eu).

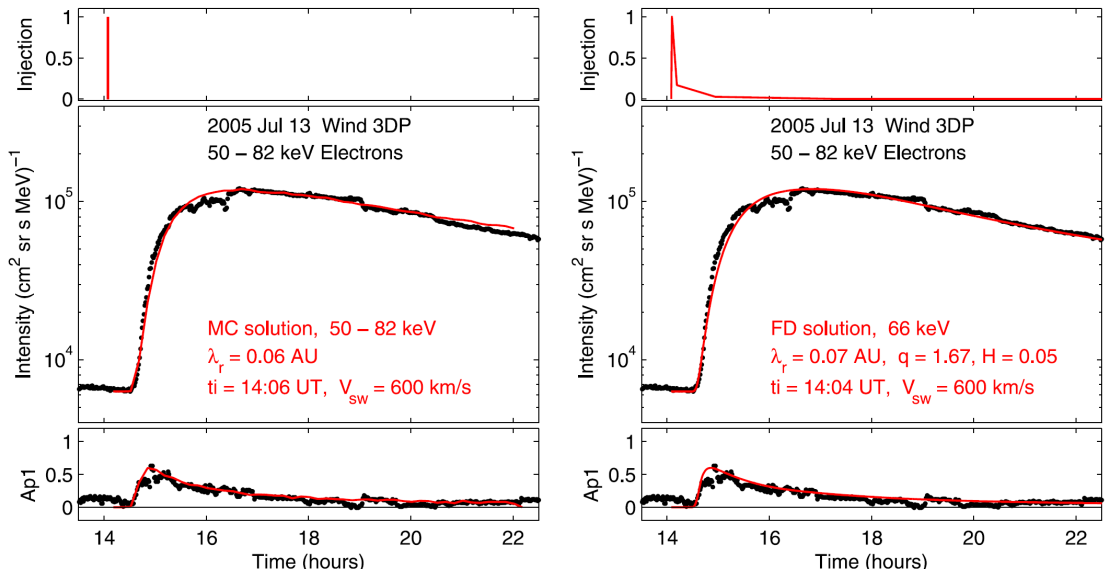

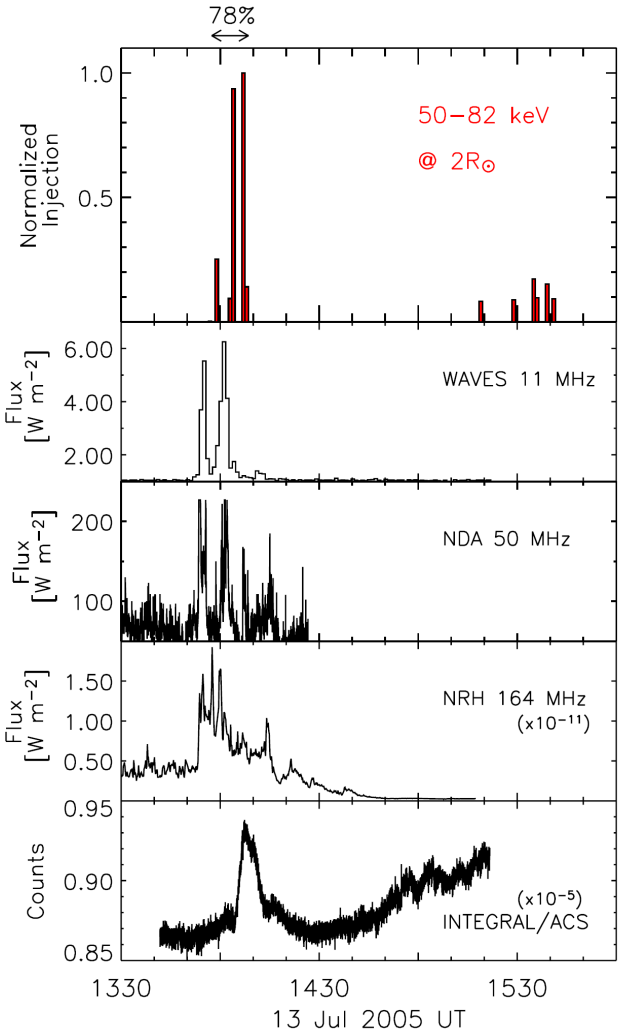

Figure 6 (top part) For each model, the top panel shows the derived injection function. (Bottom part) From top to bottom: Normalized electron injection profile (red histogram) inferred from Wind/3DP observations using an inversion approach; light curves from WAVES, NDA, NRH and INTEGRAL/ACS shifted -500 s for direct comparison with the injection profile (adapted from Malandraki et al., 2012).

Impact of the large-scale IMF structure on SEP event profiles

Tan et al. (2012) examined two large SEP events, which occurred inside Magnetic Clouds (MCs) during the solar cycle 23: the 1998 May 2 and 2002 April 21 events. The parent (S15W15) flare and CME onset of the first SEP event occurred at May 2 13:26 UT and 13:29 UT, respectively. Note that hereafter the light-travel time of 8.3 minutes from the Sun to the Earth has been subtracted from the electromagnetic radiation observation time at 1 AU. The parent (S14W84) flare and CME onset of the second SEP event occurred at April 21 00:51 UT and 01:08 UT, respectively. While the onset of the two SEP events examined was inside a MC, the onset times in the May and April event were close to the start and center of the MC interval (see Figure 8). The upper panels of Figure 7 present pitch-angle spectrograms of 66 keV electrons as deduced from the Wind/3DP/SST electron data, which display the temporal variation of their directional intensities as a function of the pitch-angle cosine (μ) of electrons for the SEP events examined. Electron data collected within each 5 minute interval are used to produce the spectrogram, and a high-order polynomial fitting is used to smooth data. In Figure 7 the presence of reflected particles is characterized by a counter-streaming electron beam with a deep depression at ~90° pitch-angles (Tan et al., 2009), where the pitch-angle scattering alone is unlikely to produce a depletion of particles. Therefore, electron reflection is observed during > 4 and > 6 hr intervals in the May and April events, respectively.

The analysis by Tan et al. (2012) showed that the PAD details of reflected electrons are found to be different. In fact, only in the first half hour since the appearance of reflected electrons are their PADs roughly similar in the two events examined. Later their PADs exhibit significant difference. This difference is illustrated in the bottom panels of Figure 7 where 10 minute cutoffs of electron pitch-angle spectrograms with background electron subtracted are shown in the event onset. For each MC two cutoffs with the time difference of ~40 minutes are displayed. Based on the IMF orientation observed during the SEP events it is concluded that the incident and reflected particles for the May event are located in the $\mu < 0$ and $\mu > 0$ regions, respectively, whereas for the April event the incident and reflected particles are in the $\mu > 0$ and $\mu < 0$ regions, respectively (Tan et al., 2012). The observations show that in the May event the peak intensity of reflected electrons is located at μ_{po}~ 0.7-0.8 as observed at 1 AU. When $\mu \rightarrow 1$, the electron intensity decreases, providing possible evidence of a loss cone. In contrast, in the April event reflected electrons are exhibited at $\mu < 0$. At the event onset the distribution of reflected electrons is roughly similar to that in the May event. However, after ~1 hr since the event onset the observed electron intensity exhibits a continuous increase at $\mu \rightarrow -1$. We carried out analysis of the observed directional intensities by the 3DP detector which showed that a loss cone is present and absent in the May and April events, respectively. Furthermore, in the May event Skoug et al. (1999) observed an IP shock that occurred at 21:23 UT on 1998 May 1. The magnetic field compression behind the shock may result in the formation of a reflecting boundary for particles (Malandraki et al., 2002).

Assuming that the first arriving particles have experienced negligible scattering (Reames, 2009a), the SRT and the path length traveled by first arriving incident (L_{oi}) and reflected (L_{or}) particles from their injection site near the Sun to the 1 AU observer can be deduced from the onset time analysis, which we carried out for both electrons and heavy ions separately, as well as the estimation of the distance between the magnetic mirroring point and the 1 AU observer in the first hour from the event onset, results (not shown) presented in detail in our work (Tan et al., 2012) for both SEP events. Comparison of the path lengths traveled by incident non-relativistic electrons with that by ~MeV nucleon^{-1} He ions in similar time intervals indicates the stability of the magnetic loops structure during a period of a few hours.

Because of the existence of reflecting boundaries of SEPs near 1 AU the observed SEP event could be additionally amplified, causing the so-called reservoir effect (Roelof et al., 1992). What we were concerned in our work was the effect of high-energy protons because of its impact on the space weather issue. In fact, high-energy protons represent 'hard' radiation that can be a significant hazard to astronauts and equipment in space, while secondary neutrons threaten passengers and crew of aircraft on polar routes. Taking into account typical proton energy spectra and the thickness of available shielding, the most important energy range for protons is from 30 to 100-200 MeV (Turner, 2006). Through the analysis of particle confinement mechanisms occurring in individual flux tubes we were able to understand the conditions that enhance the duration of high-energy proton intensities in different magnetic field topologies. We have noted that the two SEP events examined have different PADs. In the May event the presence of a loss cone in the PAD indicates that the magnetic mirror only reflects SEPs outside the loss cone back to 1 AU, whereas SEPs inside the loss cone would be lost during their further transport process. On the contrary, in the April event with $\mu_{loss} \rightarrow -1$, almost all particles could be reflected back to 1 AU. Therefore, we should expect a smaller characteristic decay time scale, τ_d, value in the May event, because the additional loss of high-energy particles inside the loss cone would result in a faster decay of particle intensities. Our expectation is consistent with the GOES 8 observations presented in Figure 8, where the high-energy electron and proton data in the May and April events are shown in the upper and lower panels, respectively. Note that the two vertical dashed lines delimit the exponential decay interval of high-energy particle intensities, which occurred after half a day and one day from the event onset in the May and April events, respectively. The τ_d value of high-energy protons in the

April event is ~1.4 times greater than that in the May event.

Based on the joint analysis of the PADs and peak intensities of electrons carried out in our work (Tan et al., 2012) it is exhibited that in the April event the reflected particles with μ_{po}~ -1 as observed at 1 AU could reach the vicinity of the Sun, implying that the magnetic loop is a magnetic bottle connected to the Sun with its two legs. In contrast, in the May event particle reflection occurs abruptly at the magnetic mirror formed by a compressed field enhancement behind an IP shock, consistent with its open field line topology (Figure 9). The so-called reservoir effect that the presence of a reflecting boundary could enhance the duration of high-energy proton intensities was found to be consistent with our observations. The relatively shorter duration of high-energy proton intensities in the May event is probably due to an additional escape of the protons inside the loss cone of the PAD.

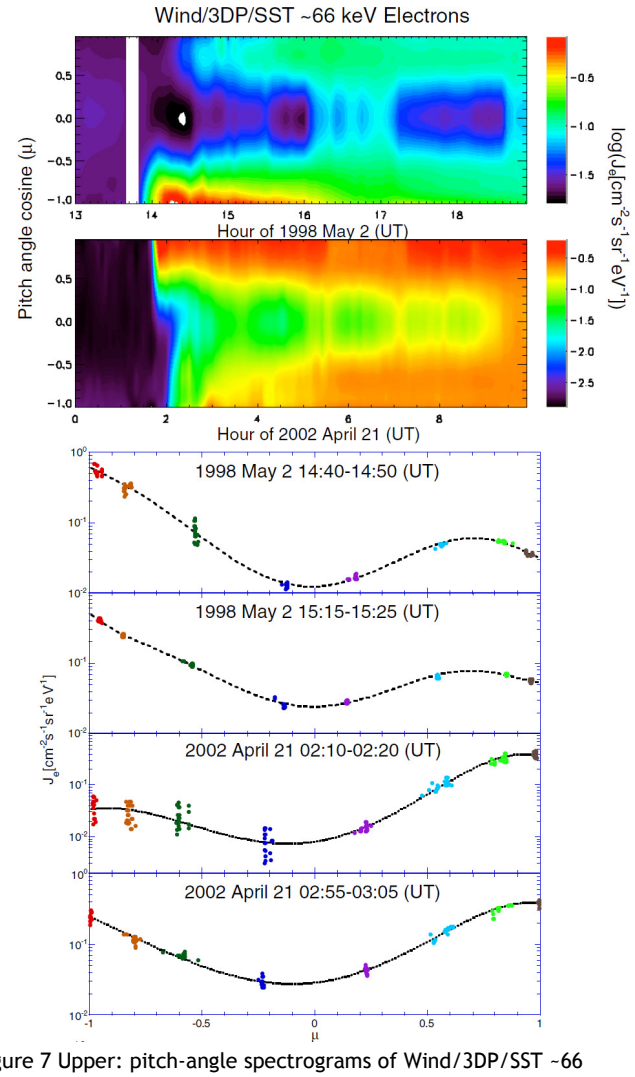

Figure 7 Upper: pitch-angle spectrograms of Wind/3DP/SST ~66 KeV electrons are displayed with a 5 minute resolution. Because of the orientation of the IMF reflected electrons are located at μ > 0 and μ < 0 regions in the 2 May 1998 and 21 April 2002 events, respectively. Lower: 10 minute cutoffs of spectrograms with background electron intensities subtracted are shown in the event onset (adapted from Tan et al., 2012).

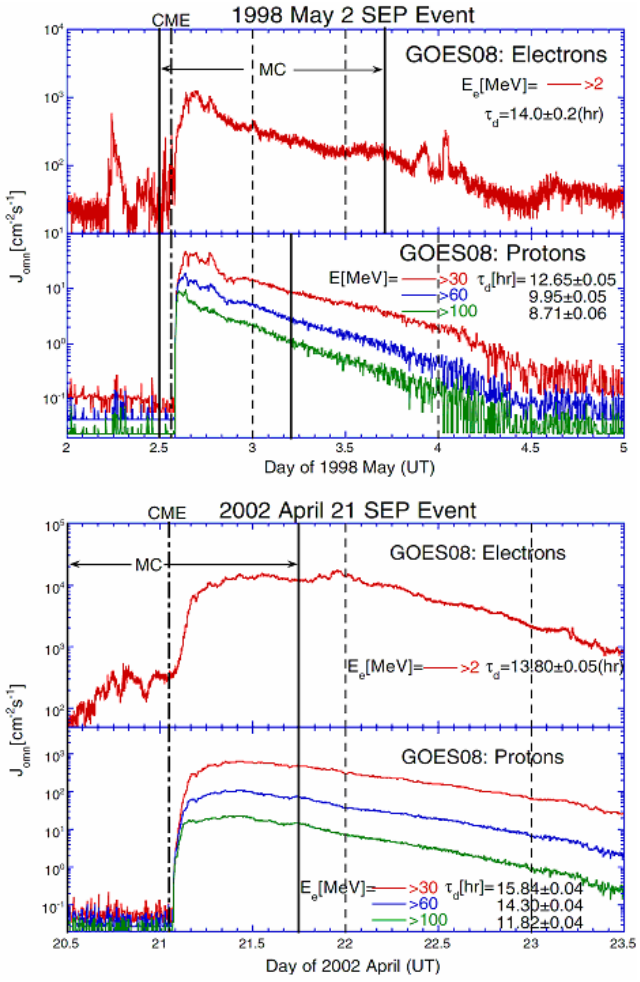

Figure 8 Omnidirectional high-energy electron and proton intensity time profiles as measured by GOES08 are shown in the upper and lower panels for the 2 May 1998 and 21 April 2002 event, respectively. The vertical dashed lines delimit the decay time of the high-energy SEP intensities (Tan et al., 2012).

Consistency of path lengths traveled by solar electrons and ions in GLEs

One of the fundamental questions in SEP investigation is the acceleration mechanism of the highest energy (GeV and above) particles (Cliver, 2008). Ions at these energies interact in the Earth's magnetosphere to produce secondary particles of sufficient intensity that can be detected by neutron monitors at ground level, causing the GLE event. Since high-energy ions represent 'hard' radiation that can be a significant hazard to astronauts and equipment in space, while secondary neutrons threaten passengers and crew of aircraft on polar routes, understanding where, when and how particle acceleration takes place in the GLE event is also an important issue in space weather forecasting (Reames 2009a, 2009b).

The onset time analysis, which is based on the scatter-free transport assumption of first arriving particles, is often used to calculate the Solar Release Time (SRT) and path length (L_o) that particles traveled from their release site near the Sun to the observed. However, there has been a long-lasting divergence

between L_o values deduced from solar electrons and ion data (e.g. Tylka et al., 2003; Mewaldt et al., 2003; see also Figure 4, this work). Using solar ion data from Wind, IMP-8, GOES, and neutron monitors, based on the onset time analysis Reames (2009a) deduced the L_{oi} value of the GLE events during solar cycle 23, which provides a fiducial mark of ion path lengths to be compared with electron observations. In the work by Tan et al. 2013 at NOA we hence calculated the L_{oe} value for those GLE events in order to compare with the L_{oi} value deduced by Reames (2009a) and possibly resolve this inconsistency. We used Wind/3DP/SST electron data and the Wind/Energetic Particle Acceleration, Composition and Transport Experiment (EPACT) (see von Rosenvinge et al. 1995)/ Low Energy Matrix Telescope (LEMT) heavy ion data. The properties of RBs, flares, and CMEs for the GLE events during solar cycle 23 were taken from the compilation of Gopalswamy et al. (2012). Tan et al. (2011) had previously noted that in the E_e range of SST the IP scattering of non-relativistic would increase with increasing E_e, thus only the IP transport of SST electrons at the lowest energy channel can be approximated to be scatter-free. Consequently, the valid L_{oeRB} value should be calculated at the lowest energy channel (E_e ~27 keV) of SST. As E_e increases the electrons scattering status would change to become diffusive, resulting in a delay of their arrival time relative to the scatter-free transport time. We thus improved the VDA, calculating the electron path length assuming that the onset time of the metric type II RB or decametric type III RB, t_{RB}, is the SRT, of non-relativistic electrons, i.e. $SRT_e = t_{RB}$. The deduction process of both L_{oe} and L_{oeRB} is shown schematically in Figure 10 (Tan et al., 2013) where the electron arrival time t is plotted versus the reciprocal of electron velocity (1/v) at the low-energy (l) and high-energy (h) points. In the figure the onset time analysis, which is based on the velocity dispersion relation, produces the solid line, whose slope ($\tan(a_o)$) is equal to the path length L_{oe}. However, since in the SST range as E_e increases the electron scattering status changes from scatter-free at lower energies to diffusive at higher energies, only at the low-energy point the electron arrival time (t_l) can be approximated to the electron arrival time under the scatter-free transport assumption. On the other hand, since at the high-energy point the first arriving electrons may not experience scatter-free transport their arrival time t_h could be delayed. Assuming t_{RB} as the SRT for the ~27 keV low-energy electrons the slope of the dashed line in Figure 10 (= $\tan(a_1)$ is the path length (L_{oeRB}) traveled by the ~27 keV electrons.

Before doing the comparison of L_{oeRB} and L_{oi} for the GLE events observed in solar cycle 23 we have checked whether any significant time variation of magnetic field topologies occurred during the event period examined. We performed such a check by using the pitch angle spectrograms observed by SST electrons and we observed one event (1998 August 24) in which the magnetic field exhibits significant variation and rejected it for our comparison analysis. For the remaining 10 GLE events (solid dot) the comparisons between L_{oeII} and L_{oi} and between L_{oeIII} and L_{oi} are shown in the upper and lower panels in Figure 11, respectively. The least-square fitting results are quite good, as the linear correlation coefficients between L_{oeRB} and L_{oi} are R ~ 0.99 in both RB = II and III cases, indicating that the probability by which L_{oeRB} and L_{oi} are uncorrelated is $P \sim 1 \times 10^{-7}$. However, from Figure 11 it is impossible to differentiate between RB = II and III because of the closeness of t_{II} and t_{III}. We hence calculate the weighted average of L_{oeRB} = (0.91 ± 0.04) L_{oi} for both RB=II and III, i.e. the deduced path lengths of ~27 keV electrons is consistent (within an error range of ± 10%) with the ion path length deduced by Reames (2009a) from the onset time analysis.

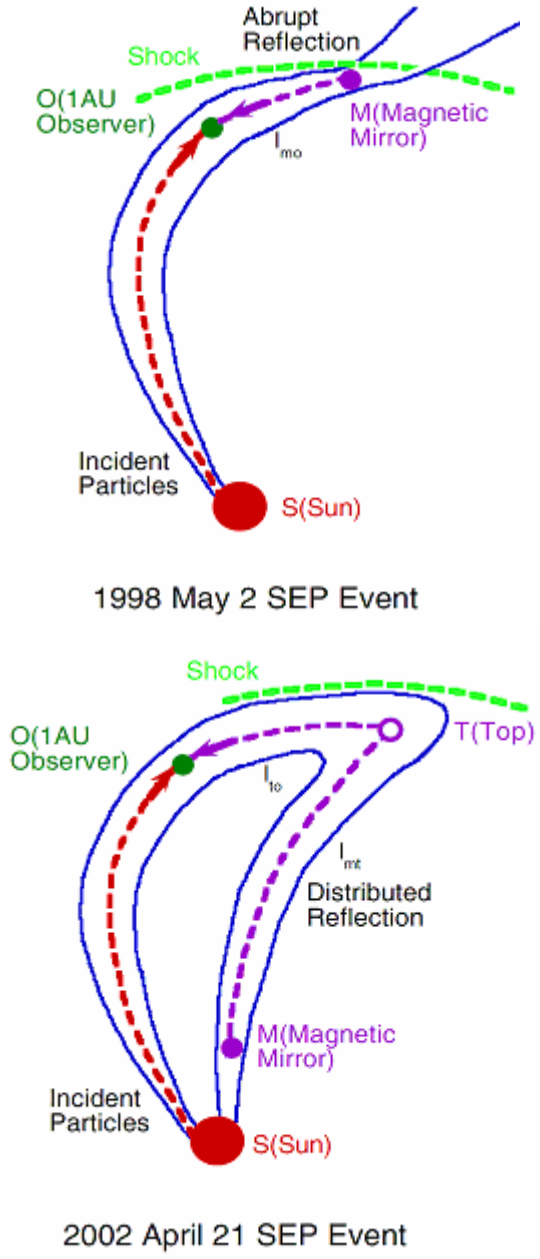

Figure 9 Schematics to show the 2D magnetic field topologies suggested for the two events under study (Tan et al., 2012).

Initial Fe/O enhancements: A Flare contribution in large, gradual SEP events?

Shocks driven by fast CMEs are the dominant particle accelerators in large, 'gradual' SEP events. In these events, the Fe/O ratio above a few MeV/nucleon sometimes shows a very strong transient enhancement at the beginning of the event, with Fe/O ~ 1, as typical of impulsive SEP events. These initial enhancements are observed when the particle intensity levels are low and rising. As intensities grow in these events, Fe/O typically decreases and approaches the nominal coronal value of ~0.1. Figure 12 shows an example of this behavior. Some researchers (e.g. Cane et al., 2003) attribute these initial enhancements to a direct flare contribution to gradual SEP events, similar to what is observed in small, impulsive events. If this interpretation is correct, we expect to see enhanced Fe/O only when the observed is magnetically-connected to the flare site. However, another explanation of initial Fe/O enhancements, which does not invoke two distinct acceleration mechanisms, is also possible. By combining high-precision observations with modeling of interplanetary transport, it was found that the temporal evolution of Fe/O, including the initial enhancements, can be generated by rigidity-dependent interplanetary transport, starting from a nominal Fe/O ~ 0.1 at the acceleration site (Ng, Reames and Tylka, 1999, 2001, 2003; see also Mason et al., 2006). The initial Fe/O enhancement observed far from the Sun occurs when

$$(M/Q)_{Fe} > (M/Q)_O,$$
$$\lambda_{mfp} < L_{path},$$

where M/Q is the ion's mass-to-charge ration, λmfp is a scattering mean free path, and Lpath is the physical path length of the magnetic field line from the acceleration site to the observer. At ~MeV/nucleon energies, average charge states in gradual events typically correspond to (M / Q)Fe ~ 4.0 and (M / Q)O ~ 2.3 (Luhn et al., 1984). Iron ions therefore have roughly twice the rigidity of oxygen ions at the same MeV/nucleon energy. Since λmfp generally increases with rigidity, the iron ions also have a longer mean free path. Furthermore, if mean free paths are small compared to Lpath, the transport process will be diffusive. As a result, the Fe intensity will rise more rapidly and reach its maximum before oxygen, corresponding to an initial enhancement in Fe/O that dies away as the event progresses. More generally, an initial Fe/O enhancement can arise whenever the pitch-angle scattering rate of Fe is significantly less than that of O.

If this transport explanation is correct, we expect to see – given sufficient instrumental collecting power- initial Fe/O enhancements even in widely separated spacecraft, at least one of which is unlikely to be magnetically connected to the flare site. We investigated this possibility at NOA (Tylka et al., 2013) using observations from the LEMT in the EPACT instrument suite on Wind and the COSPIN/LET instrument onboard Ulysses. Both instruments provided Fe and O intensities at ~5 MeV/nucleon but with geometry factors of 51 and 0.58 $cm^2\ sr^{-1}$, for LEMT and LET, respectively. Sensitivity is thus limited by LET. We therefore surveyed LET observations for 1997-2006, looking for events with an initial Fe/O > 0.8 and sufficient ion statistics in 12-hour bins to follow the evolution in the ratio over at least 2 days. During this time Wind was generally at L1, while Ulysses was at > 1.5 AU and in orbit that carried it high above the ecliptic plane. We identified two events SEP events in this manner, associated with CMEs that erupted on 15 August 2001 and 26 December 2001. Both 2001 events were cleanly observed by LEMT.

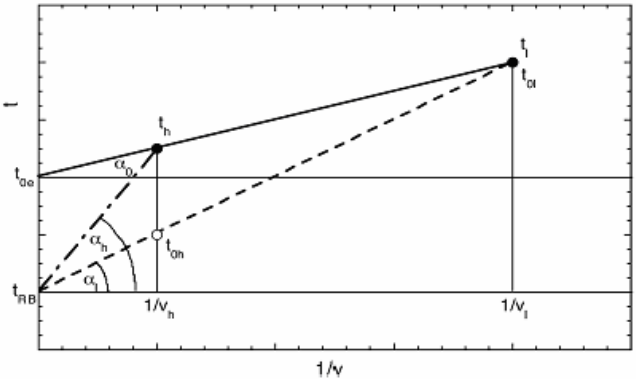

Figure 10 Electron path length calculation using VDA. The subscripts l and h denote the low-energy and high-energy points, respectively. SRT_e deduced from the onset time analysis and the onset time of the RBs are denoted by t_{oe} and t_{RB}, respectively (Tan et al., 2013) .

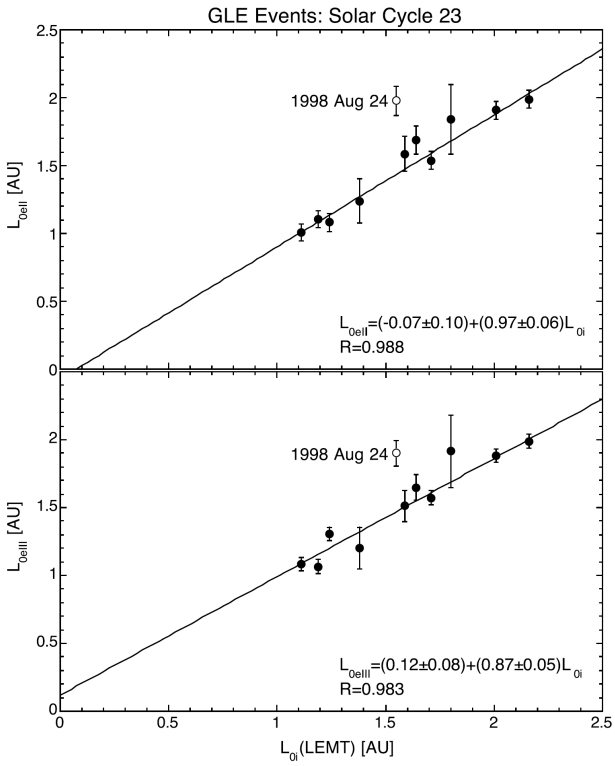

Figure 11 Electron path lengths L_{oeII} (upper) and L_{oeIII} (lower) deduced under the assumption of $SRT_e = t_{RB}$, where RB = II or III are plotted vs. the ion path length L_{oi} deduced by Reames (2009a) from the onset time analysis (Tan et al., 2013).

The left-hand panels of Figure 12 show the hourly averaged Fe and O intensities and Fe/O ratio observed by LEMT at 5 – 10 MeV/nucleon in 26 December 2001 event. This event is an exceptionally clean example of the behavior we have investigated in our study (Tylka et al., 2013). The Fe/O values are measured with high statistical precision. Over the first 12 hours of the event, the Fe/O falls by more than an order of magnitude, from above the average 'impulsive; value to near the nominal 'gradual' value. The Fe and O intensities show a rapid rise from very low background levels prior to the event. The Fe intensity peaks ~4 hours before the O intensity, whose continued rise then drives the fall of the Fe/O ratio. This event is an ideal candidate for this study first because the associated flare was at W54 heliolongitude, close to the nominal footpoint of the Sun-Earth magnetic field line, making this a good opportunity for seeing a direct flare component. Second, this event was also a GLE, the kind of event in which some researchers have also provided a 'hybrid' nature, with an initial flare component in ~ GeV protons followed by a second component from the CME-driven shock (Vashenyuk, Balabin, and Gvozdevsky, 2009; McCracken, Moraal, and Stoker, 2008). Finally the event was also clearly observed by Ulysses. At the time of this event, Ulysses had just completed its passage over the north pole of the Sun and was located at 68° N heliographic latitude and at 2.54 AU radial distance from the Sun.

The right-hand panels of Figure 12 show the Ulysses/LET profiles of Fe and O intensities and the Fe/O ratio at 5.0-10.0 MeV/nucleon, the same energy range as provided by Wind/LET. 12- hour averages were used for the Ulysses data, both for statistical reasons and because temporal evolution occurs more slowly at farther distance from the Sun. The Ulysses intensity profiles show the same qualitative behavior as at Wind, with the Fe and O intensities rising smoothly from immeasurably low background levels. Fe reaches its maximum intensity before the O intensity just as observed at L1. Although the Ulysses measurements have much less statistical precision, evolution like that at L1, is clearly evident.

We next consider the locations of the L1 and Ulysses magnetic footpoints relative to the flare site. The left panel of Figure 13 shows the solar wind speeds observed by ACE at L1 and by Ulysses during the event. Ulysses resides in a high-speed stream; L1 does not, a difference which is evidence that the L1 and Ulysses had difference magnetic footpoints at the Sun. The right panel of Figure 13 shows a synoptic map of the Sun from observations by the Extreme ultraviolet Imaging Telescope (EIT) on the SOHO spacecraft for the Carrington rotation containing the 26 December 2001 event. The yellow point marks the source region of the associated flare. The white circles mark the footpoints of the magnetic field lines that connected the Sun to L1 and to Ulysses at the start of the SEP event. These footpoint locations were calculated using the observed solar wind speeds and the Potential Field Source Surface (PFSS) model (Schatten, Wilcox and Ness, 1969, Wang and Sheeley, 2006). For the events in the study we estimate the uncertainties as ± 15°.

We calculated that the angular separation between the flare location and the L1 footpoint is 35° (12° in longitude) (see also Table 2 of Tylka et al., 2013). The angular separation between the flare and the Ulysses footpoint is 74° (68° in longitude). Thus, it is reasonable to classify L1 as 'well connected' to the flare. However, this is probably not tenable for Ulysses. In addition, the angular separation of the L1 and Ulysses footpoints is 101° (56° in longitude). If both initial enhancements were ascribed to a direct flare contribution, this is the minimum angular range which the flare particles must have been distributed.

Figure 14 presents another event in which transient Fe/O enhancements are seen both at L1 and at Ulysses. This event is the well-known 16 August 2001 'backside' event which has been associated with a source region at W180-195 (Cliver et al., 2005). Background levels prior to the event at L1 were much larger than the December event. Nevertheless, the onset and initial Fe/O enhancement are clear at L1. Ulysses was at 64° N heliographic latitude and at 1.65 AU radial distance from the Sun. Ulysses ion statistics are poor at the onset, and the Fe/O enhancement becomes clearly observable only ~24 hours into the event. Figure 15 shows the solar wind speed profiles at the time of this event and the relevant SOHO/EIT Carrington map. Although the solar wind speed profiles are highly dynamic, it is clear that L1 and Ulysses were in different solar wind streams for at least the first 30 hours of the event. Footpoint locations at the start of the event are shown in the Carrington map. The angular separation between the flare location and the L1 footpoint is 126° (124° in longitude). The angular separation between the flare and the Ulysses footpoint is 112° (97° in longitude), In this event, neither L1 nor Ulysses is magnetically well-connected to the flare site.

An initial flare contribution to a large, gradual SEP event is a logical hypothesis. However, it is a logical error to cite an initial Fe/O enhancement as evidence for a flare contribution. Given that initial Fe/O enhancements are seen at widely separated spacecraft, even when one or both is not magnetically well-connected to the flare site, it is likely that the initial Fe/O enhancement is generally a transport effect. On the other hand, the possibility of a direct flare contribution component is certainly not ruled out by this study. Measurements of iron charge states in the first few hours of the gradual event might serve to do so. To date, however, instruments for measuring charge states in the ~MeV/nucleon energy have had too little collecting power to extract meaningful measurements during the small intensities at the onset of the event.

Our observations are also particularly relevant to the controversy concerning how SEPs reach high heliolatitude. One school of thought claims that the CME-driven shocks are broad in latitude as well as longitude; when the shock intercepts the Sun-Ulysses field line, shock-accelerated particles are injected on to that field line, along which they travel outward to

Ulysses (Malandraki et al., 2009). The observations presented in this work are consistent with this scenario.

Summary and Perspectives on SEP Research

This paper presents a review of the results and contributions on space weather research from the SEP event perspective, carried out at NOA in Greece within the SEPServer and COMESEP (FP7-EU) projects. In coordination with the PI teams, NOA directly contributes key SEP interplanetary data to SEPServer, as well as catalogues of SEP events observed in the 3-D Heliosphere, all now available to the scientific community. Malandraki et al. (2012) carried out the first SEPServer comparative analysis for the case study of 13 July 2005 event, with data-driven analysis and simulation-based data analysis capable of deconvolving the effects of interplanetary transport and solar injection from SEP observations, and a comparison of the results with the electromagnetic signatures. This work also describes in detail the data products and analysis strategies, as well as the tools and results provided on the web server of the project, greatly facilitating the investigation of SEPs and their origin by the scientific community.

The results of our SEP research at NOA were used in order to test validate the test particle SEP model developed and integrated within the SEP forecasting tools of the First European Alert System, the COMESEP Space Weather Alert System (http://www.comesep.eu/alert/). We found that the so-called reservoir effect that the presence of a reflecting boundary could enhance the duration of high-energy proton intensities is consistent with our observations and the existence of a loss cone in the trapping configuration of the particles proved to be critical for the observed relatively shorter duration of the high-energy proton intensities which constitute an important significant radiation hazard to astronauts and equipment in space and to the passengers of high-altitude aircraft flying polar routes. Investigation of the source and acceleration of the SEP events showed that shocks driven by fast CMEs are the dominant particle accelerators in large gradual SEP events, even in the cases when a transient Fe/O enhancement is initially observed. These observations demonstrate that an initial Fe/O enhancement cannot be cited as evidence for a direct flare component. Instead, initial Fe/O enhancements are better understood as a transport effect, driven by the different mass-to-charge ratios of Fe and O.

Acknowledgements

This work has been supported by the European Union Seventh Framework Programmes (FP7/2007-2013) under Grant Agreement No. 263252 [COMESEP] and No. 262773 [SEPServer]. My special thanks are due to Prof. L. J. Lanzerotti (Ulysses/HI-SCALE), Dr. R. G. Marsden (Ulysses/COSPIN/LET), Dr. R. G. Gold & Dr. D. K. Haggerty (ACE/EPAM) and Dr. R. A. Mewaldt (ACE/SIS, STEREO/LET) and their teams for providing their instrument data to NOA.

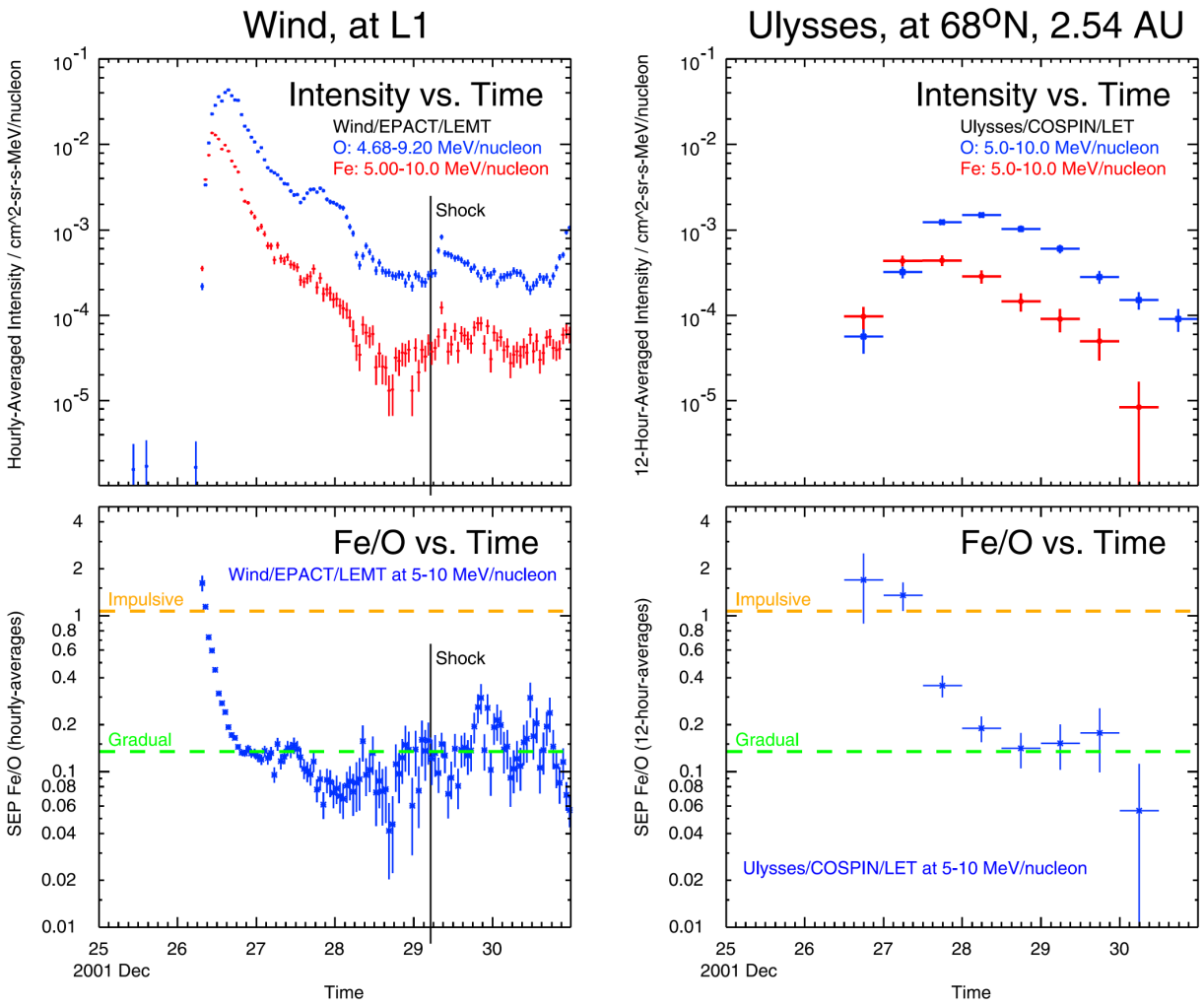

Figure 12 Fe and O intensities (top panels) from Wind at L1 (left panels) and Ulysses (right panels) for the SEP event of 26 December 2001 (Tylka et al., 2013).

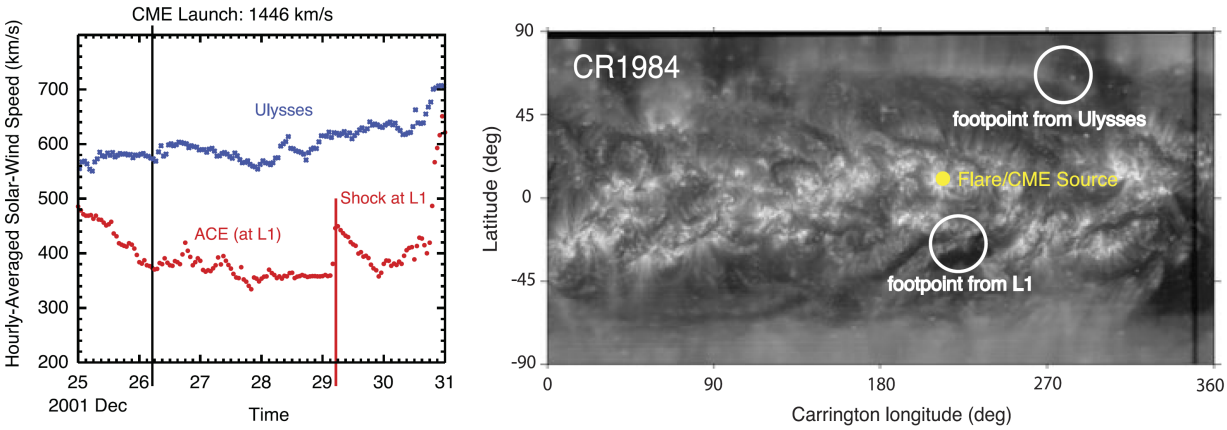

Figure 13 Figure 13: Left: Solar wind speed as observed at Ulysses (blue) and by ACE at L1 (red) during the 26 December 2001 event. Right: Synoptic map of the Sun from SOHO/EIT observations for the Carrington rotation containing the 26 December 2001 event (Tylka et al., 2013).

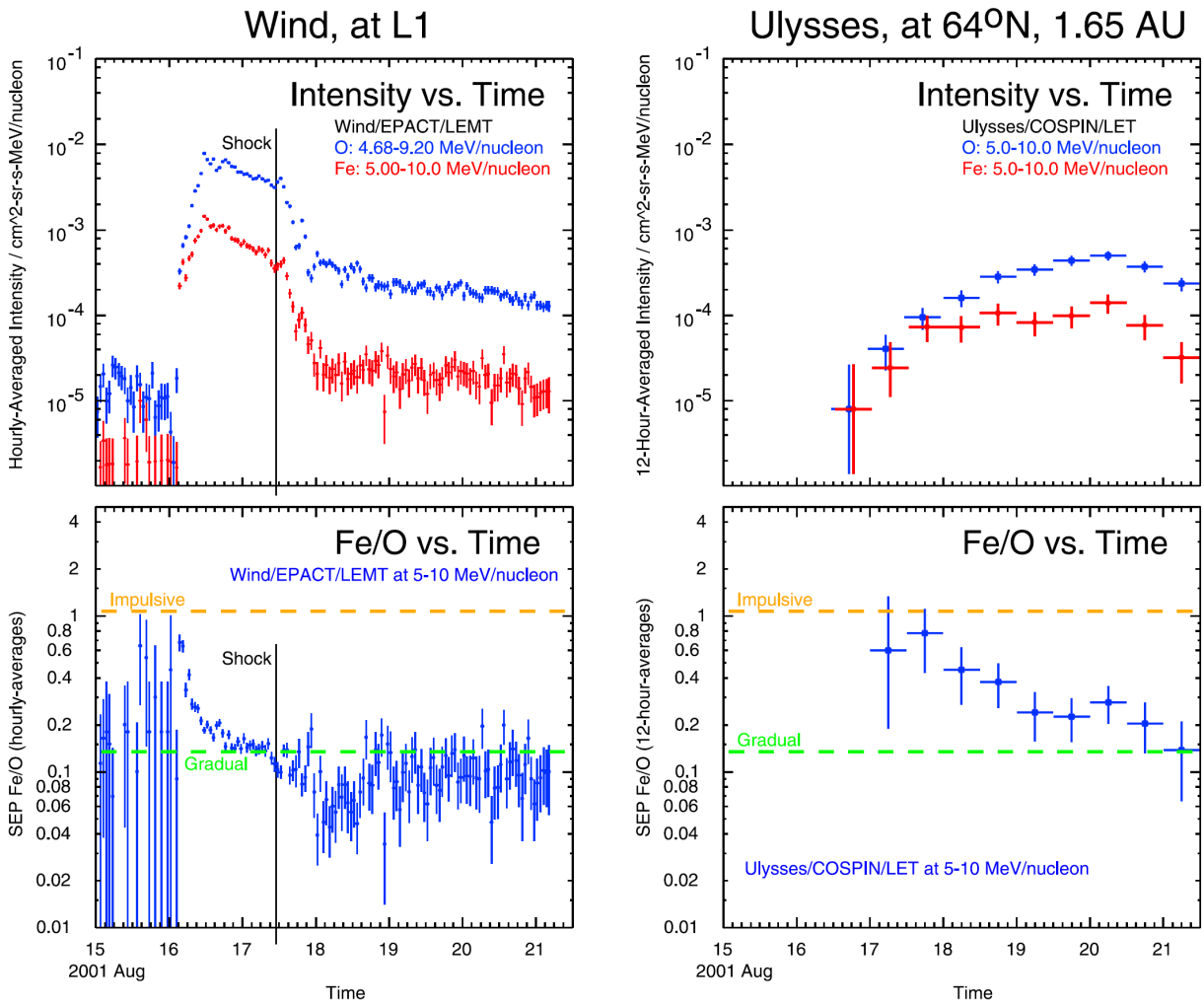

Figure 14 Like Figure 12, but for the 16 August 2001 event.

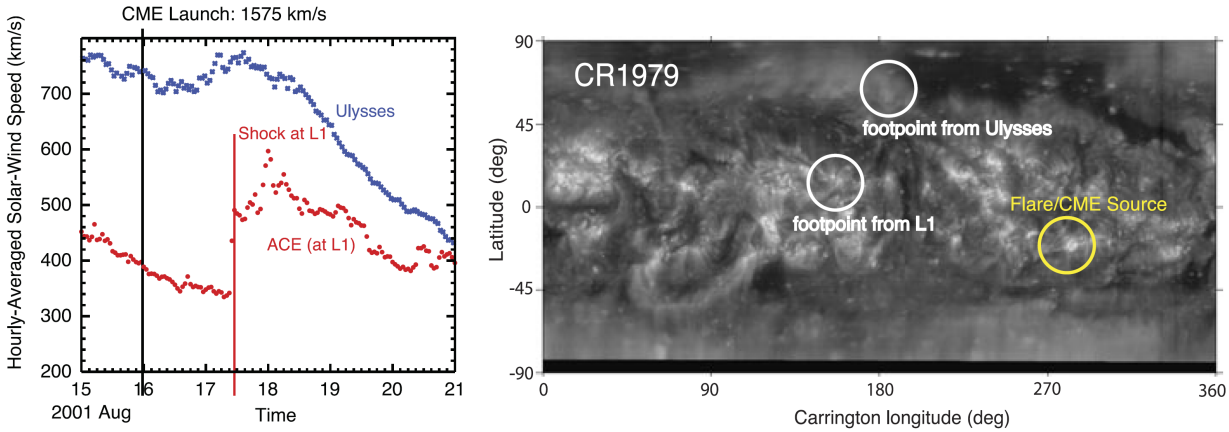

Figure 15 Like Figure 13, but for the 16 August 2001 event.

References

Agueda, N., Vainio, R., Lario, D., and Sanahuja, B.: 2008, Astrophys. J., 675, 1601, doi:10.1086/527527.

Bucík, R., Mall, U., Gómez-Herrero, R., Korth, A., and Mason, G.M.: 2009, Sol. Phys., 259, 361, doi:10.1007/s11207-009-9415-9.

Cane, H.V., von Rosenvinge, T.T., Cohen, C.M.S., and Mewaldt, R.A.: 2003, Geophys. Res. Lett., 30, 8017, doi:10.1029/2002GL016580.

Cliver, E.W., Thompson, B.J., Lawrence, G.R., Zhukov, A.N., Tylka, A.J., Dietrich, W.F., et al.: 2005, Proc. of the 29th Int. Cosmic Ray Conf., Pune, India, 1, 121.

Cliver, E.W.: 2008, in Gopalswamy, N. & Webb, D.F., 'Universal Heliophysical Processes, IAU Symp. 257, Cambridge University Press, p. 401.

Crosby, N.B., Veronig, A., Robbrecht, E., Vrsnak, B., Vennerstrom, S., Malandraki, O., et al. and COMESEP Consortium: 2012, in Q. Hu, G. Li, G.P. Zank, O. Verkhoglyadova, J.H. Adams (ed.), SPACE WEATHER: THE SPACE RADIATION ENVIRONMENT, American Institute of Physics Conference Series 1500, 159, doi:10.1063/1.4768760.

Dresing, N., Gómez-Herrero, R., Klassen, A., Heber, B., Malandraki, O., Dröge, W., and Kartavykh, Y.: 2014, A&A, 567, idA27, 15pp., doi:10.1051/0004-6361/201423789.

Dröge, W.: 2003, Astrophys. J., 589, 1027, doi:10.1086/374812.

Galvin, A.B., Kistler, L.M., Popecki, M.A., Farrugia, C. J., Simunac, K. D. C., Ellis, L., Möbius, E., et al.: 2008, Space Sci. Rev., 136, 437, doi:10.1007/s11214-007-9296-x.

Gold, R.E., Krimigis, S.M., Hawkins, S.E.III, Haggerty, D.K., Lohr, D.A., Fiore, E., Armstrong, et al.: 1998, Space Sci. Rev., 86, 541, doi:10.1023/A:1005088115759.

Gómez-Herrero, R., Malandraki, O.E., Dresing, N., et al.: 2011, J. Atmos. Sol-Terr. Phys., 73, 551, doi:10.1016/j.jastp.2010.11.017.

Gopalswamy, N., Xie, H., Yashiro, S., et al.: 2012, Space Sci. Rev., 171, 23, doi:10.1007/s11214-012-9890-4.

Heber, B., Agueda, N., Heyderickx, D., Klein, K.-L., Malandraki, O.E., et al., 2013, Proc. 33rd Int. Cosmic Ray Conf., Rio de Janeiro, Brazil, No. 0761.

Huttunen-Heikinmaa, K., Valtonen, E., and Laitinen, T.: 2005, Astron&Astrophys, 442, 673.

Kallenrode, M.-B, and Wibberenz, G.: 1991, Astrophys. J., 376, 787.

Kartavykh, Y.Y., Dröge, W., Klecker, B., et al.: 2007, Astrophys. J., 671, 947, doi:10.1086/522687.

Krucker, S., and Lin, R.P.: 2000, Astrophys. J. Lett. 542, L61.

Lanzerotti, L.J., Gold, R.E., Anderson, K.A., et al.: 1992, Astron&Astrophys., 92, 349.

Leske, R.A., Cohen, C.M.S., Mewaldt, R.A., et al.: 2011, Proc. of the 32nd Int. Cosmic Ray Conf., Beijing, China, 10, 200.

Lin, R.P., Anderson, K.A., Ashford, S., et al.: 1995, Space Sci. Rev., 71, 125, doi:10.1007/BF00751328.

Luhn, A., Klecker, B., Hovestadt, D., et al.: 1984, Adv. Space Res., 4(2-3), 161, doi:10.1016/0273-1177(84)90307-7.

Malandraki, O.E., Sarris, E.T., Lanzerotti, L.J., Trochoutsos, P., , et al.: 2002, J. Atmos. Solar-Terr. Phys., 64, 517.

Malandraki, O.E., Marsden, R.G., Tranquille, C., , et al.: 2007, J. Geophys. Res., 112, A06111, doi:10.1029/2006JA011876.

Malandraki, O.E., Marsden, R.G., Tranquille, C., , et al.: 2008, Annales Geophys., 26, 1029.

Malandraki, O.E., Marsden, R.G., Lario, D., et al.: 2009, Astrophys. J., 704, 469, doi:10.1088/0004-637X/704/1/469.

Malandraki, O.E., Agueda, N., Papaioannou, A., et al.: 2012, Sol. Phys. 281, 333, doi:10.1007/s11207-012-0164-9.

Malandraki, O.E.: 2013, Proceedings of the 11th Hellenic Astronomical Conference, Athens, Greece, http://www.helas.gr/conf/2013/

Mason, G.M., Desai, M.I., Cohen, C.M.S., Mewaldt, R.A., Stone, E.C., and Dwyer, J.R.: 2006, Astrophys. J. Lett., 647, L65, doi:10.1086/507469.

McComas, D. J., Bame, S.J., Barker, P. , et al.: 1998, Space Sci. Rev., 86, 563.

McCracken, K.G., Moraal, H., Stoker, P.H.: 2008, J. Geophys. Res., 113, A12101, doi:10.1029/2007JA012829.

Mewaldt, R.A., Cohen, C.M.S., Haggerty, D.K., et al.: 2003, Proc. of the 28th Int. Cosmic Ray Conf., Tokyo, Japan, 6, 3313.

Mewaldt, R.A., Cohen, C.M.S., Cook, W.R., et al.: 2008, Space Sci. Rev., 136, 285, doi:10.1007/s11214-007-9288-x.

Ng, C.K., Reames, D.V., and Tylka, A.J.: 1999, Geophys. Res. Lett., 26, 2145.

Ng., C.K., Reames, D.V., and Tylka, A.J.: 2001, Proc. of the 27th Int. Cosmic Ray Conf., Hamburg, 8, 3140.

Ng., C.K., Reames, D.V., and Tylka, A.J.: 2003, Astrophys. J., 591, 461.

Papaioannou, A., Malandraki, O.E., Dresing, N., et al.: 2014, Astron& Astrophys. 569, A96, doi:10.1051/0004-6361/201323336.

Reames, D.V.: 2009a, Astrophys. J., 693, 812.

Reames, D.V.: 2009b, Astrophys. J., 706, 844.

Reames, D.V.: 2013, Space Sci. Rev., 175/1-4, 53.

Roelof, E.C.: 1969, Lectures in High-Energy Astrophysics, NASA SP-199, 111.

Roelof, E.C., Gold, R.E., Simnett, G.M. , et al.: 1992, Geophys. Res. Lett., 19, 1243, doi:10.1029/92GL01312.

Richardson, I. G.: 2004, Space Sci. Rev., 111, 267

Schatten, K.H., Wilcox, J.M., Ness, N.F..: 1969, Sol. Phys., 6, 422.

Simpson, J.A., Anglin, J.D., Balogh, A., et al .: 1992, Astron&Astrophys, 92, 365.

Skoug, R.M., Bame, S.J., Feldman, W.C., Gosling, , et al.: 1999, Geophys. Res. Lett., 26, 161, doi:10.1029/1998GL900207.

Stone, E.C., Cohen, C.M.S., Cook, W.R., et al.: 1998, Space Sci. Rev., 86, 357, doi:10.1023/A:1005027929871.

Tan, L.C., Reames, D.V., Ng, C.K., Saloniemi, O., and Wang, L.: 2009, Astrophys. J., 701, 1753, doi:10.1088/0004-637X/701/2/1753.

Tan, L.C., Reames, D.V., Ng, C.K., Shao, X., and Wang, L.: 2011, Astrophys. J, 728, 133, 10.1088/0004-637X/728/2/133.

Tan, L.C., Malandraki, O.E., Reames, D.V., Ng, C.K., et al.: 2012, Astrophys. J., 750, 146, doi:10.1088/0004-637X/750/2/146.

Tan, L.C., Malandraki, O.E., Reames, D.V., , et al.: 2013, Astrophys. J., 768, 68, doi:10.1088/0004-637X/768/1/68.

Turner, R.E.: 2006, in N. Gopalswamy et al. (ed.), Solar Eruptions and Energetic Particles, Geophys. Monogr. Ser., Vol. 165, Washington DC, AGU), p. 367.

Tylka, A.J., Cohen, C.M.S., Dietrich, W.F., et al.: 2003, Proc. of the 28th Int. Cosmic Ray Conf., Tokyo, Japan, 6, 3305.

Tylka, A.J., Malandraki, O.E., Dorrian, G., Ko, Y.-K., Marsden, R. G., Ng, C. K., and Tranquille, C.: 2013, Sol. Phys., 285, 251.

Vainio, R., Valtonen, E., Heber, B., Malandraki, O. et al: 2013, J. Space Weather Space Clim. 3, A12, doi:10.1051/swsc/2013030.

Vashenyuk, E.V., Balabin, Yu V, Gvozdevsky, B.B.: 2009, Proc. of the 31st Int. Cosmic Ray Conf. Lodz, Poland, N. 1304.

Von Rosenvinge, T.T., Barbier, L.M., Karsch, J., et al.: 1995, Space Sci. Rev., 71, 155 doi:10.1007/BF00751329.

Wang, Y.-M., and Sheeley, N.R. Jr.: 2006, Astrophys. J., 653, 708.